

# Improvement of stability of Nb<sub>3</sub>Sn superconductors by introducing high specific heat substances

X Xu<sup>1</sup>, P Li<sup>1</sup>, A V Zlobin<sup>1</sup> and X Peng<sup>2</sup>

<sup>1</sup> Fermi National Accelerator Laboratory, Batavia, IL 60510, U.S.A

<sup>2</sup> Hyper Tech Research Incorporated, 539 Industrial Mile Road, Columbus, OH 43228, U.S.A

E-mail: xxu@fnal.gov

## Abstract

High- $J_c$  Nb<sub>3</sub>Sn conductors have low stability against perturbations, which accounts for the slow training rates of high-field Nb<sub>3</sub>Sn magnets. While it is known that adding substances with high specific heat ( $C$ ) into Nb<sub>3</sub>Sn wires can increase their overall specific heat and thus improve their stability, there has not been a practical method that is compatible with fabrication of long-length conductors. In this work, we put forward a scheme to introduce such substances to distributed-barrier Nb<sub>3</sub>Sn wires, which adds minimum difficulty to the wire manufacturing process. Multifilamentary wires using a mixture of Cu and high- $C$  Gd<sub>2</sub>O<sub>3</sub> powders have been successfully fabricated along this line. Measurements showed that addition of Gd<sub>2</sub>O<sub>3</sub> had no negative effects on RRR or non-Cu  $J_c$ , and that flux jumps were remarkably reduced, and minimum quench energy (MQE) values at 4.2 K, 14 T were increased by a factor of three, indicating that stability was significantly improved. We also discussed the influences of positioning of high- $C$  substances and their thermal diffusivity on their effectiveness in reducing superconductor temperature rise against perturbations. Based on these results we proposed an optimized conductor architecture to maximize the effectiveness of this approach.

**Keywords:** Nb<sub>3</sub>Sn Superconductor, Stability, Specific Heat Capacity.

## 1. Introduction

Instability of superconductors due to perturbations is a key issue for design and operation of superconducting magnets. Efforts in developing Nb<sub>3</sub>Sn dipole and quadrupole magnets in recent years show that Nb<sub>3</sub>Sn magnets are less stable and have slower training rates than NbTi magnets: most Nb<sub>3</sub>Sn dipole and quadrupole magnets require long trainings (e.g., tens of quenches) to reach 80-90% of their short sample limits [1-3]. Magnet training is a very costly and time-consuming procedure; thus, it is very desirable to minimize it by improving stability of superconducting magnets.

It is well established that for a superconductor with high critical current density  $J_c$ , improved intrinsic stability can be achieved by reducing filament size, increasing temperature margin, increasing specific heat, and dynamic cooling [4]. For modern high- $J_c$  Nb<sub>3</sub>Sn conductors used to generate high magnetic fields, there is limited room for further improvement of the first two factors. As to dynamic stabilization, Nb<sub>3</sub>Sn coils are usually impregnated with epoxy, which has low thermal diffusivity, while common heat disturbances such as flux jumps and wire motions release substantial heat in short periods (0.01-1 ms), causing adiabatic temperature rise before heat can be conducted away. On the other hand, increasing specific heat of superconductors could not only lead to significant intrinsic stability gain, but also help to reduce sensitivity to external perturbations (i.e., improving energy margins against quenches). Due to the low specific heat  $C$  of Nb<sub>3</sub>Sn conductors at their operational temperatures, even a tiny heat disturbance with energy of  $Q$  would cause a dramatic temperature rise  $\Delta T$ , as  $\Delta T = Q/C$ . Therefore, improving conductor specific heat is one of the most promising approaches to improving magnet stability.

The specific heat of superconductors (such as NbTi and Nb<sub>3</sub>Sn) and matrix (Cu) can hardly be significantly increased; however, there is a class of materials with high specific heat at low

temperatures, and addition of such substances to a superconducting wire in a proper architecture can improve its overall  $C$  [5-7]. Experiments showed that the high specific heat of these substances was not fully utilized when they were added to epoxy, which has low thermal diffusivity [8]; however, when they were directly added into superconducting wires (e.g., being placed between the Ta barrier and the outside Cu sheath in bronze-process  $Nb_3Sn$  wires [9], or being filled into holes that were drilled in Cu matrix in NbTi billets [10]), the minimum quench energies (MQE) of these conductors were significantly increased (e.g., by factors of 5-7 as reported in [9]). Nevertheless, these schemes of adding high- $C$  substances significantly increased billet fabrication difficulty and undermined wire drawability, making it difficult to obtain practical long-length wires. Furthermore, such schemes cannot be applied to distributed-barrier  $Nb_3Sn$  wires, which have high  $J_c$ s and are the conductors of choice for building high-field (10-16 T) accelerator magnets.

As discussed above, the key difficulty for practical use of this increasing- $C$  technique lies in proper modification of the conductor design and fabrication to incorporate high- $C$  substances without introducing much manufacturing difficulty. To solve this problem, we developed a technique to introduce high- $C$  substances to distributed-barrier  $Nb_3Sn$  wires. To produce a present-day distributed-barrier  $Nb_3Sn$  wire, a number of hexagonal  $Nb_3Sn$  subelements (each with its own Cu sheath) and Cu rods are stacked into a Cu can to compose a billet, which is then drawn to wires at final sizes. Taking advantage of the stacking process, our scheme simply replaces some Cu rods and  $Nb_3Sn$  subelements with Cu tubes filled with high- $C$  powders. This approach adds minimum difficulty to the wire manufacturing process.

Moreover, because high- $C$  substances are typically ceramic compounds with very low thermal diffusivities, we also propose using a mixture of Cu and high- $C$  powders instead of pure

high- $C$  powder. This brings two advantages: 1) Cu can enhance thermal conduction among the high- $C$  particles, and 2) distributing ductile Cu in high- $C$  particles (which are typically hard and non-deformable) benefits wire drawing and makes it easier to obtain small subelement size without filament breakage. The ideal structure for such a mixture is that Cu particles form a continuous network, which divides high- $C$  powders into small islands (*i.e.*, no larger than a few microns): in such a case, heat conduction distance in each high- $C$  island is small, so it can absorb heat effectively in short periods.

## 2. Experimental

A 61-restack regular control wire and a high- $C$  wire with filaments containing mixture of Cu and  $Gd_2O_3$  powders (with the Cu: $Gd_2O_3$  weight ratio of 1:2) were fabricated. Their  $Nb_3Sn$  subelements were based on the “tube type” technology: a Cu-encased Sn rod was inserted into a Nb-7.5wt.%Ta tube to form a subelement – for such a subelement after heat treatment part of the Nb-7.5wt.%Ta (~25-30% of the whole subelement area [11]) would remain as barrier against Sn leakage into the Cu matrix. Both wires were drawn to 1.0 mm and 0.7 mm diameters (with subelement sizes of ~100  $\mu m$  and ~70  $\mu m$ , respectively) with lengths over 100 meters without any breakage, with SEM images shown in figure 1. The high- $C$  filaments were placed both in the center and at the corners so that each  $Nb_3Sn$  subelement was not far from a high- $C$  filament. The Cu/non-Cu ratios for the control wire and the high- $C$  wire were ~1.0 and ~1.1, respectively (the high- $C$  filaments were counted as “Cu”).  $Gd_2O_3$  was used for this work due to its commercial availability and high  $C$  at low temperatures. Cu powder of -325 mesh and nano  $Gd_2O_3$  powder were used.

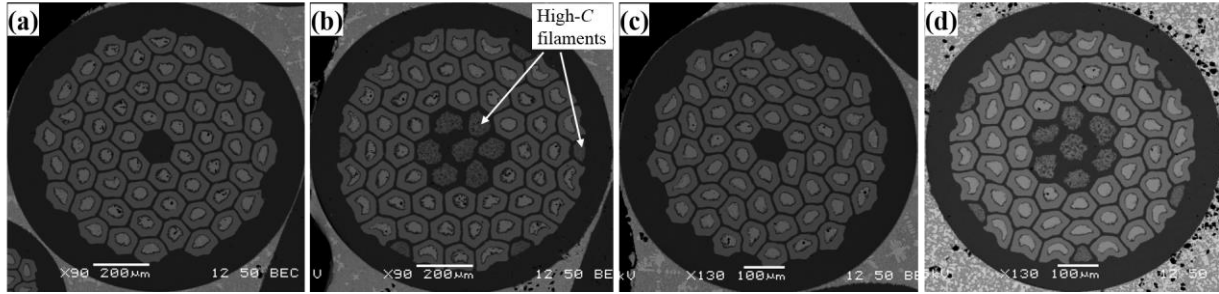


Figure 1. SEM images of (a) the control wire at 1.0 mm, (b) the high-*C* wire at 1.0 mm, (c) the control wire at 0.7 mm, and (d) the high-*C* wire at 0.7 mm.

All wires (about 25 cm piece length) were heat treated at 625 °C for 250 hours and at 640 °C for 200 hours in an argon-flowing furnace. After heat treatment, the samples used for measurements and SEM studies were cut from the middle of the reacted wires.

For transport tests, each straight segment of ~5 cm was measured with field perpendicular to wire axis and voltage tap separation was 10 mm, with a criterion of 1  $\mu\text{V}/\text{cm}$  used to determine its critical current ( $I_c$ ). Residual resistivity ratio (RRR) measurements were done on ~6 cm long straight samples, and the RRR values were determined as the resistance at 300 K over that at 20 K. Magnetization vs magnetic field ( $M$ - $B$ ) loops were measured using the Vibrating Sample Magnetometer (VSM) option of a 9 T “physical property measuring system” (PPMS). Each ~4 mm long wire sample was oriented with its axis perpendicular to the applied field. The heat capacities of samples were measured in a PPMS from 2 K to 20 K at 0 T and 9 T. Minimum quench energies were measured on 1.0 mm wires. Strain gauges (WK-09-125BT-350 from Micro-Measurements) were glued to the samples using GE varnish, with the gauge patterns (~4 mm in length and ~1.5 mm in width) centered on the wires and their long sides parallel to the wire axes. After complete curing of GE varnish, the sample and the strain gauge were covered

with a thick layer (~1 mm) of Stycast. A 400 W KEPCO power supply provided excitation voltage to the strain gauge. Using a LabView DAQ program, we can generate  $\mu\text{s}$ -wide pulse output from the power supply and measure the voltage across the strain gauge. With the  $I_c$  of the sample first measured, a constant bias current below  $I_c$  was applied to the sample and heat pulses were fired using the strain gauge. In this study, the duration of the heat pulses was fixed at 100  $\mu\text{s}$ . A separate quench protection monitored the voltage across the sample and shut down the power supply if the quench threshold was reached. By gradually increasing the pulse power (in a step of 0.03  $\mu\text{J}$  when approaching the critical energy), the critical energy that induced a quench was defined as the MQE of the sample.

### 3. Results

The RRR values for the control wire and the high- $C$  wire after reaction at 625 °C for 250 hours were 107 and 271 for the 1.0 mm wires and 23 and 34 for the 0.7 mm wires, respectively, indicating that adding such high- $C$  filaments did not undermine RRR. The 4.2 K, 15 T  $J_c s$  normalized to the  $\text{Nb}_3\text{Sn}$  subelement areas of the control wire and the high- $C$  wire after reaction at 625 °C for 250 hours were 720 and 750  $\text{A}/\text{mm}^2$ , respectively, which were similar. The heat capacity of a high- $C$  filament after heat treatment at 625 °C for 250 hours was measured in a PPMS and the calculated volumetric specific heat capacities of  $\text{Gd}_2\text{O}_3$  at zero field and 9 T are shown in figure 2, along with the literature data for Cu and  $\text{Nb}_3\text{Sn}$ . It is seen that addition of  $\text{Gd}_2\text{O}_3$  is more efficient in increasing specific heat at 2 K than at 4.2 K. At 0 T, 2 K the ratio of the specific heat of  $\text{Gd}_2\text{O}_3$  to that of Cu is nearly 1000, but it drops to only ~170 at 4.2 K. This is consistent with previous report that the specific heat of  $\text{Gd}_2\text{O}_3$  with cubic crystal structure peaks at ~2 K [12].

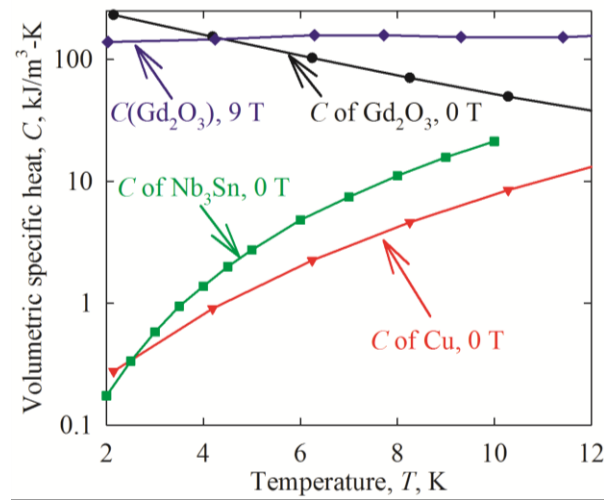


Figure 2. The volumetric specific heat of Gd<sub>2</sub>O<sub>3</sub>, Cu, and Nb<sub>3</sub>Sn.

The measured  $M$ - $B$  loops at 4.2 K of 0.7 and 1.0 mm wires after reaction at 625 °C for 250 hours are shown in figure 3. Compared with the control wires, the wires with high- $C$  filaments had smaller flux jump amplitudes, indicating that the stability was improved. Larger flux jump amplitudes lead to higher energy release and temperature rise [13], and are very undesirable. It is also interesting to note that Gd<sub>2</sub>O<sub>3</sub> has a large magnetic susceptibility at 4.2 K [14] and thus had non-negligible magnetization contributions to the  $M$ - $B$  curves.

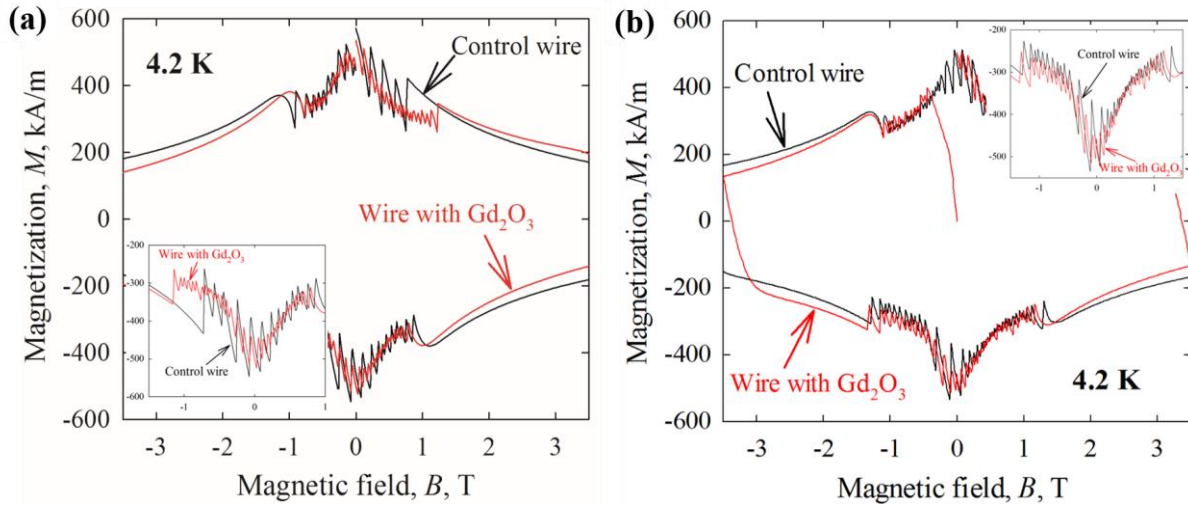


Figure 3.  $M$ - $B$  loops of (a) 0.7 mm and (b) 1.0 mm wires (with magnetizations normalized to the non-Cu volumes). The inserts show blow-ups of the flux jump regions.

The MQE values of both 1.0 mm wires after reaction at 640 °C for 200 hours were measured and the results are shown in figure 4. The  $I_{cs}$  at 4.2 K, 14 T of the control wire and the high- $C$  wire were 444 and 426 A (with non-Cu  $J_{cs}$  of 1150 and 1180 A/mm<sup>2</sup>), respectively. From figure 4 it can be seen that the MQE values of the high- $C$  wire were over three times higher than those of the control wire.

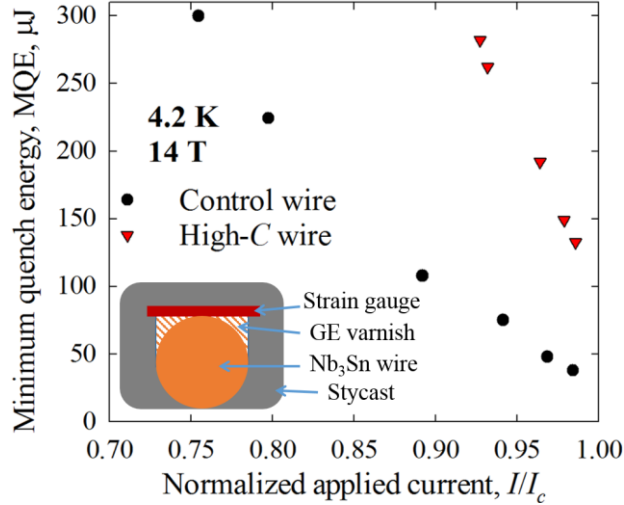


Figure 4. MQE values of the control wire and the high- $C$  wire measured at 4.2 K, 14 T, with the insert showing a simple schematic diagram for measuring MQE.

#### 4. Discussion

The reduced flux jumps in figure 3 reflect improvement of stability in the low field range ( $< 2$  T), while the increased MQE values in figure 4 demonstrate the improvement of conductor stability at high fields against external perturbations while carrying high currents. These results show that the stability of  $\text{Nb}_3\text{Sn}$  conductors has been improved over a wide range of magnetic fields by introducing high- $C$  filaments. It should be noted that increase of  $C$  of  $\text{Nb}_3\text{Sn}$  conductors may lead to some change of normal zone propagation velocity, which needs further studies.

For the addition of high- $C$  substances to improve the stability of superconductors, it is crucial to study their effectiveness in absorbing heat. We believe the effectiveness of high- $C$  substances depends on two factors: their positions in a conductor, as well as their thermal diffusivities. In superconducting coils heat is mostly generated by perturbations outside conductors (e.g., due to epoxy cracking) and transfer to the Cu matrix before diffusing into superconducting

subelements. It is easy to understand that placing the high- $C$  layer between the heat-exposed Cu matrix and the  $\text{Nb}_3\text{Sn}$  subelements is the most effective way for intercepting the heat before it diffuses into  $\text{Nb}_3\text{Sn}$  superconductors, while placing the high- $C$  substances on the opposite side of the  $\text{Nb}_3\text{Sn}$  layer with respect to the heat source would have much less effect in preventing temperature rise in  $\text{Nb}_3\text{Sn}$ .

Based on the above considerations, a feasible wire design to maximize the effectiveness of this technique is to place the high- $C$  filaments in the outmost layer of the subelement array, a schematic shown in figure 5 (b) (with a present-day  $\text{Nb}_3\text{Sn}$  wire in figure 5a). In this structure, the Cu sheath between the high- $C$  filaments still allows for some heat diffusion from the outside Cu to inner-row subelements. In this case the effectiveness is sensitive to the thermal diffusivity of the high- $C$  filaments: high thermal diffusivity is important to ensure quick heat absorption by the high- $C$  substance. For example, if their thermal diffusivity is very low, considerable portion of the heat can still diffuse into inner-row subelements because the time constant for heat absorption by the high- $C$  filaments is too large.

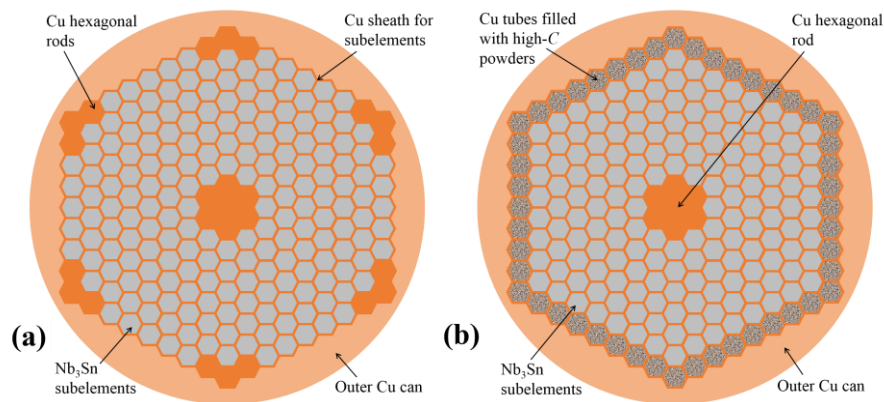


Figure 5. Schematics of cross sections of (a) a regular  $\text{Nb}_3\text{Sn}$  wire and (b) a wire with high- $C$  filaments in the outermost layer.

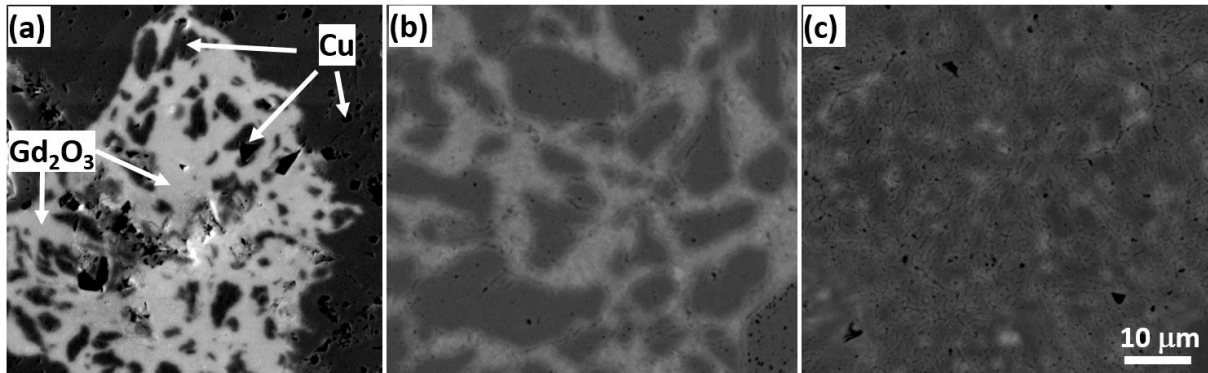


Figure 6. SEM images of Cu and Gd<sub>2</sub>O<sub>3</sub> mixtures with Cu/Gd<sub>2</sub>O<sub>3</sub> weight ratios of (a) 1:2, (b) 2:1, and (c) 4:1. In these images Cu appears as the dark phase and Gd<sub>2</sub>O<sub>3</sub> appears bright.

Figure 6 (a) shows SEM image of a high-*C* filament used in the high-*C* wire in figure 1. We notice that Cu only formed isolated islands in Gd<sub>2</sub>O<sub>3</sub> instead of forming the desired continuous thermal transport network. In such a case, the low thermal diffusivity of Gd<sub>2</sub>O<sub>3</sub> does not allow heat to diffuse far into the high-*C* filaments in short periods; as a result, it is very likely that certain amount of Gd<sub>2</sub>O<sub>3</sub> in the center of high-*C* filaments was not yet activated to absorb heat before flux jumps or quenches occurred. Figure 6 (a) indicates that the Cu/Gd<sub>2</sub>O<sub>3</sub> ratio (1:2) used in the high-*C* wire in this work might not be high enough. To determine the minimum amount of Cu powder to form a continuous heat transfer network, filaments with higher Cu/Gd<sub>2</sub>O<sub>3</sub> ratios (2:1 and 4:1) were fabricated, with SEM images shown in Figure 6 (b) and (c), respectively. It can be seen that Cu/Gd<sub>2</sub>O<sub>3</sub> ratio of 2:1 still did not lead to a continuous Cu network, while the ratio of 4:1 was too high. Thus, we expect that the optimal Cu/Gd<sub>2</sub>O<sub>3</sub> weight ratio may be around 3:1 – this of course also depends on Cu and Gd<sub>2</sub>O<sub>3</sub> particle sizes and mixing techniques. It is expected that new conductors with optimized Cu and Gd<sub>2</sub>O<sub>3</sub> ratio and mixing and proper

positioning of high- $C$  filaments will have significantly superior stability compared with the high- $C$  wire shown in this work.

With a Cu/Gd<sub>2</sub>O<sub>3</sub> weight ratio of 3:1, it is estimated that for a Nb<sub>3</sub>Sn conductor with 217 subelements and the outmost-layer subelements replaced by high- $C$  filaments as shown in figure 5 (b), the Gd<sub>2</sub>O<sub>3</sub> takes ~2 vol.%, and the fraction of Nb<sub>3</sub>Sn subelements depends on the Cu/non-Cu ratio design, while the rest is Cu (including the Cu matrix and the Cu powder in high- $C$  filaments). With 2 vol.% of Gd<sub>2</sub>O<sub>3</sub> added, the overall specific heat of a Nb<sub>3</sub>Sn conductor can be improved by factors of ~20 and ~3.4 at 2 K and 4.2 K, respectively. It is worth pointing out that addition of high- $C$  filaments does not necessarily lead to decrease in Nb<sub>3</sub>Sn fraction and thus engineering  $J_c$ , because we can reduce the Cu matrix volume to compensate the addition of high- $C$  filaments. For addition of 2 vol.% of Gd<sub>2</sub>O<sub>3</sub>, 1 kg of Nb<sub>3</sub>Sn wire needs 17 grams of Gd<sub>2</sub>O<sub>3</sub>. Based on our investigations on the market, the price of Gd<sub>2</sub>O<sub>3</sub> is significantly lower than the current price of Nb<sub>3</sub>Sn conductors. In addition, fabrication of such high- $C$  filaments is based on the common powder-in-tube technique. Thus, it is expected that the prices of such new high- $C$  conductors should not be noticeably higher than those of present-day Nb<sub>3</sub>Sn conductors. Apart from Gd<sub>2</sub>O<sub>3</sub>, it is also useful to explore other high- $C$  substances that have not only high  $C$ , but also high thermal diffusivity, such as PrB<sub>6</sub>, which may work more effectively than Gd<sub>2</sub>O<sub>3</sub>.

## 5. Conclusions

An innovative technique was developed to introduce high- $C$  substances to distributed-barrier Nb<sub>3</sub>Sn superconductors without negative impacts on wire manufacturing. Conductors have been successfully fabricated with Gd<sub>2</sub>O<sub>3</sub> addition without any issues. It was found that RRR or non-

Cu  $J_c$  was not negatively affected by the addition of Gd<sub>2</sub>O<sub>3</sub>. Measurements at 4.2 K showed that flux jumps at low fields were remarkably suppressed and MQE values at high fields were increased by a factor of three, indicating that the wire stability was significantly improved due to addition of such high- $C$  substances. The conductors in this work still have a lot of room for improvement. With further optimization of wire design, this new type of Nb<sub>3</sub>Sn conductors can be industrially produced and used for large-scale applications to reduce or eliminate training of Nb<sub>3</sub>Sn magnets.

### Acknowledgements

This work was supported by Fermi Research Alliance, LLC, under contract No. DE-AC02-07CH11359 with the U.S. Department of Energy. The heat capacity measurements were conducted in the Center for Nanoscale Materials, Argonne National Laboratory, which was supported by the U.S. Department of Energy, Office of Science, Office of Basic Energy Sciences, under Contract No. DE-AC02-06CH11357.

### References

- [1]. Feher S et al. 2007 Development and Test of LARP Technological Quadrupole (TQC) Magnet *IEEE Trans. Appl. Supercond.* **17**, 1126-9
- [2]. Chlachidze G et al. 2013 Test of Optimized 120 -mm LARP Nb<sub>3</sub>Sn Quadrupole Coil Using Magnetic Mirror Structure *IEEE Trans. Appl. Supercond.* **23**, 4001605
- [3]. Zlobin A V et al. 2015 11-T Twin-Aperture Nb<sub>3</sub>Sn Dipole Development for LHC Upgrades *IEEE Trans. Appl. Supercond.* **25**, 4002209
- [4]. Wilson M N 1983 Superconducting Magnets *Oxford University Press*, 139–141.
- [5]. Hancox R 1968 Enthalpy stabilized superconducting magnets *IEEE Trans. Magn.* **4**, 486-8
- [6]. Russenblum S, Sheinberg H and Steyert W A 1977 High specific heat metals for use in superconducting magnets *IEEE Trans. Magn.* **MAG-13**, 834-5
- [7]. Kwasnitza K, Barbisch B and Hulliger F 1983 Metallic materials for superconductor stabilization with very high specific heat and good thermal conductivity *Cryogenics* **23**, 649-52

- [8]. Alekseev P A et al. 2006 Influence of high heat capacity substances doping on quench currents of fast ramped superconducting oval windings *Cryogenics* **46**, 252-5
- [9]. Keilin V E et al. 2009 Considerable stability increase of Nb<sub>3</sub>Sn multifilamentary wire internally doped with a large heat capacity substance (PrB<sub>6</sub>) *Supercond. Sci. Technol.* **22**, 085007
- [10]. Keilin V E et al. 2012 Stability of superconducting coils made of NbTi wires internally doped with large heat capacity Gd<sub>2</sub>O<sub>3</sub> powder *Supercond. Sci. Technol.* **25**, 115017
- [11]. Xu X, Sumption M D, Bhartiya S, Peng X and Collings E W 2013 Critical current densities and microstructures in rod-in-tube and Tube Type Nb<sub>3</sub>Sn strands – Present status and prospects for improvement *Supercond. Sci. Technol.* **26** 075015
- [12]. Stewart G R, Barclay J A and Steyert W A 1979 The specific heat of C-phase Gd<sub>2</sub>O<sub>3</sub> *Solid State Commun.* **29**, 17-9
- [13]. Xu X, Sumption M D and Collings E W 2014 Influence of heat treatment temperature and Ti doping on low-field flux jumping and stability in (Nb-Ta)<sub>3</sub>Sn strands *Supercond. Sci. Technol.* **27**, 095009
- [14]. Miller A E, Jelinek F J, Gschneidner K A and Gerstein B C 1971 Low-Temperature Magnetic Behavior of Several Oxides of Gadolinium *J. Chem. Phys.* **55** 2647-8